

## Kinetics of glass transition and crystallization in multicomponent bulk amorphous alloys

ZHUANG Yanxin (庄艳歆), ZHAO Deqian (赵德乾),  
ZHANG Yong (张勇), WANG Weihua (汪卫华)  
& PAN Mingxiang (潘明祥)

Institute of Physics, Chinese Academy of Sciences, Beijing 100080, China

Correspondence should be addressed to Wang Weihua (email: whw@aphy.iphy.ac.cn)

Received November 5, 1999

**Abstract** Differential scanning calorimeter (DSC) is used to investigate apparent activation energy of glass transition and crystallization of Zr-based bulk amorphous alloys by Kissinger equation under non-isothermal condition. It is shown that the glass transition behavior as well as crystallization reaction depends on the heating rate and has a characteristic of kinetic effects. After being isothermally annealed near glass transition temperature, the apparent activation energy of glass transition increases and the apparent activation energy of crystallization reaction decreases. However, the kinetic effects are independent of the pre-annealing.

**Keywords:** bulk amorphous alloys, glass transition, crystallization, kinetics.

Bulk amorphous alloys (BAAs) are one of the most interesting fields in materials sciences and physics due to their excellent glass forming ability (GFA), wide supercooled liquid region (SLR), high thermal stability against crystallization and unique properties<sup>[1-4]</sup>. The crystallization of the BAAs, greatly different from that of conventional amorphous alloys is characterized by multi-step crystallization, high nucleation rates and low growth rates, thus enabling us to make a more direct investigation of the time-dependent nucleation<sup>[5]</sup>. Crystallization studies of the BAAs are of importance in understanding the mechanisms of phase transformations far from equilibrium, evaluating GFA of the melts and producing bulk nanocrystalline materials or amorphous/nanocrystalline composites by controlled crystallization. Generally, structural relaxation induced by atomic arrangements in the process of low temperature annealing of amorphous alloys not only leads to changes in most physical properties, but also has obvious effects on subsequent crystallization<sup>[6, 7]</sup>. Up to now, the crystallization features of these BAAs and effects of local atomic structure on glass transition (GT) and crystallization are not understood very well, and there is no detailed work on crystallization kinetics of the BAAs. The crystallization kinetics of BAAs in different states can provide essential parameters of controlled crystallization and information on the essence of the excellent GFA and effects of structural relaxation on subsequent crystallization. On the other hand, the GT is one of the most important and intensively investigated topics in the amorphous alloys. However, there still lacks a comprehensive understanding of the GT. In this paper, the GT and crystallization of the as-prepared  $Zr_{41}Ti_{14}Cu_{12.5}Ni_{10-x}Fe_xBe_{22.5}$  ( $x = 0, 2, 5$ ) BAAs and the  $Zr_{41}Ti_{14}Cu_{12.5}Ni_{10}Be_{22.5}$  BAAs annealed near glass transition temperature ( $T_g$ ) are studied, and relation of GFA with the crystallization kinetics and effects of structural relaxation

induced by pre-annealing on crystallization kinetics are discussed.

## 1 Experiments

Ingot with nominal desired compositions were prepared by melting a mixture of 99.9% pure elements in titanium-gettered Ar atmosphere arc furnace, then remelted in vacuum-sealed quartz tubes and quenched in water to get amorphous rods with a diameter of 16mm. The amorphous nature as well as the homogeneity of the as-prepared rod was ascertained with X-ray diffraction (XRD) and a transmission electron microscope (TEM). 0.5 mm thick slices were cut from the amorphous rod and ground for annealing and DSC measurements. The samples were annealed in a furnace with a vacuum of  $2.0 \times 10^{-3}$  Pa and temperature accuracy of  $\pm 0.5$  K. The XRD measurements were processed by a Mac Science MXP-AHF18 diffractometer with  $\text{Cu K}\alpha$  radiation. The differential scanning calorimeter (DSC) measurements were carried out under a purified argon atmosphere in a Perkin Elmer DSC7 with the heating rate,  $\phi$ , ranging from 2.5 to 80 K/min. Calorimeter was calibrated with high purity indium and zinc at various heating rates. The values of the  $T_g$ , the onset crystallization temperature ( $T_x$ ) and the crystallization peak temperature ( $T_{pi}$ ) were determined from the DSC traces with an accuracy of  $\pm 1$  K.

The apparent activation energy ( $E$ ) and frequency factor ( $\nu_0$ ) of the GT and the main crystallization reactions were determined by the Kissinger method under non-isothermal condition<sup>[8]</sup>:

$$\ln \frac{\theta^2}{\phi} = \frac{E}{k_B \theta} + \ln \frac{E}{k_B \nu_0}, \quad (1)$$

where  $\theta$  is  $T$  or  $T_{pi}$ ,  $k_B$  is the Boltzmann constant;  $E$  and  $\nu_0$  can be obtained from the slope and intercept of plots of  $\ln(\theta^2/\phi)$  versus  $1/\theta$ , respectively.

## 2 Results

The glass transition behavior and crystallization of BAAs is closely related to alloys compositions. The obtained values of  $T_g$ ,  $T_x$ ,  $T_{pi}$  and SLR,  $\Delta T = T_x - T_g$  for as-prepared  $\text{Zr}_{41}\text{Ti}_{14}\text{Cu}_{12.5}\text{Ni}_{10-x}\text{Fe}_x\text{Be}_{22.5}$  ( $x = 0, 2, 5$ ) BAAs determined at a heating rate of 20 K/min are listed in table 1.  $\Delta T$  can be used to evaluate the GFA. The BAAs with larger  $\Delta T$  is of better GFA<sup>[9]</sup>.  $\Delta T$  decreases with increasing Fe content from 0 to 5at.%, indicating that the GFA of the  $\text{Zr}_{41}\text{Ti}_{14}\text{Cu}_{12.5}\text{Ni}_{10-x}\text{Fe}_x\text{Be}_{22.5}$  ( $x = 0, 2, 5$ ) alloys decreases when Fe content increases. The result is in agreement with that of experimental observation. Fig. 1 shows the DSC traces obtained from the as-prepared  $\text{Zr}_{41}\text{Ti}_{14}\text{Cu}_{12.5}\text{Ni}_{10}\text{Be}_{22.5}$  BAA at different heating rates. The  $T_g$ ,  $T_x$ ,  $T_{pi}$  and SLR of the BAA are shifted to higher temperature with increasing heating rate. Not only crystallization but also GT display dependence on the heating rate during continuous heating, meaning that both of GT and crystallization have significant kinetic effects. Similar trend exists in the DSC traces for the other two BAAs ( $x = 2,$

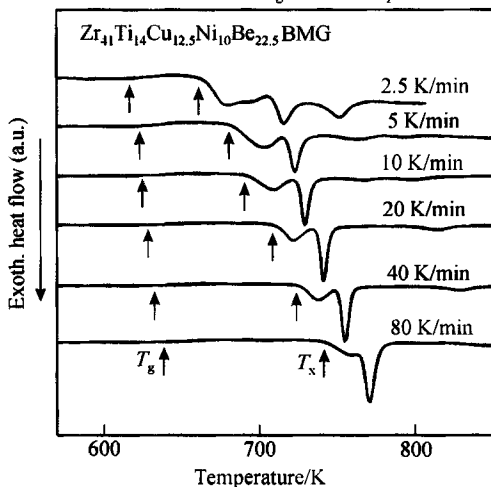


Fig. 1. DSC traces for the as-prepared  $\text{Zr}_{41}\text{Ti}_{14}\text{Cu}_{12.5}\text{Ni}_{10}\text{Be}_{22.5}$  bulk amorphous alloys at different heating rates.

$\text{Zr}_{41}\text{Ti}_{14}\text{Cu}_{12.5}\text{Ni}_{10-x}\text{Fe}_x\text{Be}_{22.5}$  ( $x = 0, 2, 5$ ) BAAs determined at a heating rate of 20 K/min are listed in table 1.  $\Delta T$  can be used to evaluate the GFA. The BAAs with larger  $\Delta T$  is of better GFA<sup>[9]</sup>.  $\Delta T$  decreases with increasing Fe content from 0 to 5at.%, indicating that the GFA of the  $\text{Zr}_{41}\text{Ti}_{14}\text{Cu}_{12.5}\text{Ni}_{10-x}\text{Fe}_x\text{Be}_{22.5}$  ( $x = 0, 2, 5$ ) alloys decreases when Fe content increases. The result is in agreement with that of experimental observation. Fig. 1 shows the DSC traces obtained from the as-prepared  $\text{Zr}_{41}\text{Ti}_{14}\text{Cu}_{12.5}\text{Ni}_{10}\text{Be}_{22.5}$  BAA at different heating rates. The  $T_g$ ,  $T_x$ ,  $T_{pi}$  and SLR of the BAA are shifted to higher temperature with increasing heating rate. Not only crystallization but also GT display dependence on the heating rate during continuous heating, meaning that both of GT and crystallization have significant kinetic effects. Similar trend exists in the DSC traces for the other two BAAs ( $x = 2,$

5), suggesting that the Fe content has a significant effect on crystallization, but cannot change the kinetic effects of GT and crystallization. The Kissinger plots of GT and the second crystallization peak for the  $Zr_{41}Ti_{14}Cu_{12.5}Ni_{10-x}Fe_xBe_{22.5}$  ( $x = 0, 2, 5$ ) BAAs are displayed in fig. 2(a) and (b). The apparent activation energy of crystallization increases with the addition of Fe element.

Table 1 Values of  $T_g$ ,  $T_x$ ,  $T_{p1}$ ,  $\Delta T$  and  $E$  for as-prepared  $Zr_{41}Ti_{14}Cu_{12.5}Ni_{10-x}Fe_xBe_{22.5}$  ( $x = 0, 2, 5$ ) BAAs and  $Zr_{41}Ti_{14}Cu_{12.5}Ni_{10}Be_{22.5}$  at different states

	$T_g/K$	$T_x/K$	$T_{p1}/K$	$T_{p2}/K$	$\Delta T/K$	$E_g/r$ (kJ/mol)	$E_{p1}/r$ (kJ/mol)	$E_{p2}/r$ (kJ/mol)
$Zr_{41}Ti_{14}Cu_{12.5}Ni_{10}Be_{22.5}$ (as-prepared)	629	710	722	741	81	559.11/0.994	192.56/0.989	267.33/0.995
$Zr_{41}Ti_{14}Cu_{12.5}Ni_8Fe_2Be_{22.5}$ (as-prepared)	627	687	701	733	60	475.00/0.994	226.66/0.999	319.85/0.998
$Zr_{41}Ti_{14}Cu_{12.5}Ni_5Fe_5Be_{22.5}$ (as-prepared)	634	687	701	736	53	604.37/0.997	266.21/0.998	332.64/0.999
$Zr_{41}Ti_{14}Cu_{12.5}Ni_{10}Be_{22.5}$ (annealed at 623 K for 2 h)	631	681	707	739	50	453.29/0.988	256.68/0.990	317.13/0.994
$Zr_{41}Ti_{14}Cu_{12.5}Ni_{10}Be_{22.5}$ (annealed at 623 K for 6 h)	632	693	715	738	61	235.98/0.986	231.62/0.984	313.87/0.995

Values of  $T_g$ ,  $T_x$ ,  $T_{p1}$  and  $\Delta T$  are measured at the heating rate of 20 K/min;  $r$  is the correlation coefficient.

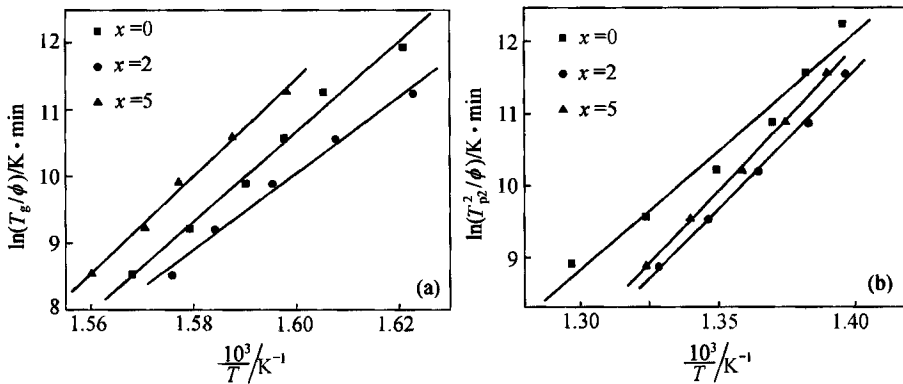


Fig. 2. Kissinger plots of glass transition (a) and second crystallization peak (b) for the as-prepared  $Zr_{41}Ti_{14}Cu_{12.5}Ni_{10-x}Fe_xBe_{22.5}$  ( $x = 0, 2, 5$ ) bulk amorphous alloys.

Fig. 3 gives the DSC traces for the as-prepared and pre-annealing  $Zr_{41}Ti_{14}Cu_{12}Ni_{10}Be_{22.5}$  alloys determined at a heating rate of 20 K/min. The pre-annealing near  $T_g$  markedly changed the crystallization behavior of the  $Zr_{41}Ti_{14}Cu_{12.5}Ni_{10}Be_{22.5}$  BAA. The values of  $\Delta T$ ,  $T_g$ ,  $T_x$  and  $T_{p1}$  for the three alloys are different, indicating that the structure change induced by pre-annealing has great effects on GT and crystallization of Zr-based BAAs. However,  $T_g$ ,  $T_x$  and  $T_{p1}$  are also shifted to higher temperature with increasing heating rate for the annealed alloys, and the kinetic feature of GT and crystallization are not changed by the structure development.  $T_g$ ,  $T_x$ ,  $T_{p1}$  and  $\Delta T$  determined at the heating rate of 20K/min are listed in table 1 together with  $E_g$  and  $E_{p1}$  evaluated from Kissinger plots for the pre-annealed  $Zr_{41}Ti_{14}Cu_{12.5}Ni_{10}Be_{22.5}$  alloys. After the BAA were annealed near  $T_g$ , the  $E_g$  decreased, while the  $E_{p1}$  first increased and then  $E_{p1}$  decreased with the annealing time.

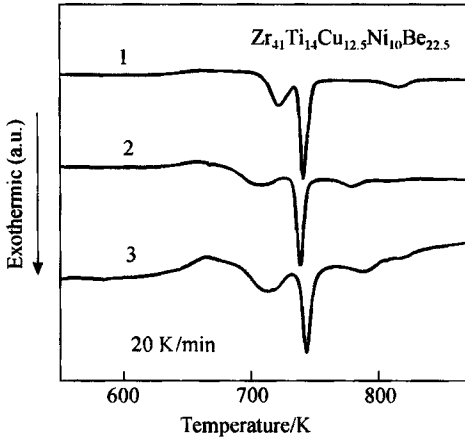


Fig. 3. DSC traces for the  $Zr_{41}Ti_{14}Cu_{12.5}Ni_{10}Be_{22.5}$  BMG at different states; 1, as-prepared; 2, annealed at 623 K for 2 h; 3, annealed at 623 K for 6 h.

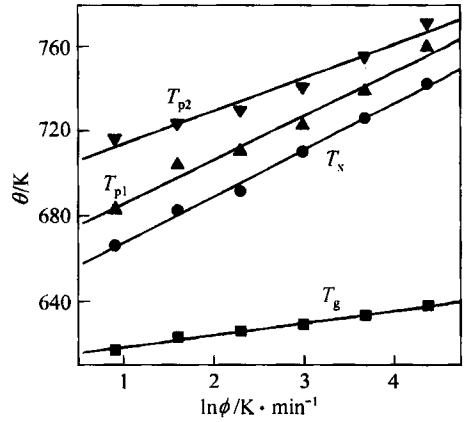


Fig. 4. Plots of  $T_g$ ,  $T_x$ ,  $T_{p1}$ ,  $T_{p2}$  vs.  $\ln\phi$  for as-prepared  $Zr_{41}Ti_{14}Cu_{12.5}Ni_{10}Be_{22.5}$  bulk amorphous alloys.

### 3 Analysis and discussion

#### 3.1 Kinetic effect of glass transition and crystallization

The results obtained above show that the  $T_g$ ,  $T_x$ ,  $T_{pi}$  and  $\Delta T$  are closely dependent on the heating rate and shifted to higher temperature with increasing heating rate for the as-prepared and pre-annealed BAAs. Fig. 4 illustrates the linear relationship of  $T_g$ ,  $T_x$ ,  $T_{p1}$  and  $T_{p2}$  with  $\ln\phi$  for as-prepared  $Zr_{41}Ti_{14}Cu_{12.5}Ni_{10}Be_{22.5}$  BAA, which can be written as

$$\theta = A_\theta + B_\theta \ln\phi. \quad (2)$$

$A_\theta$  and  $B_\theta$  are constants. The  $A_\theta$  and  $B_\theta$  for as-prepared and pre-annealing BAAs are listed in table 2. As displayed in fig. 4 and table 2, the crystallization has stronger dependence on the heating rate than that of GT, meaning that kinetic effect of crystallization is more obvious than that of GT. Pre-annealing changes the values of  $B_\theta$ , suggesting that the kinetic effect of GT increases and the kinetic effect of crystallization decreases after annealing in the SLR.

The values of specific heat capacity of the BAAs transit from the glass states to the supercooled liquid. For example, the changes of specific heat capacity are 0.312 J/g·K for as-prepared  $Zr_{41}Ti_{14}Cu_{12.5}Ni_{10}Be_{22.5}$  BAA, 0.316 J/g·K for as-prepared  $Zr_{41}Ti_{14}Cu_{12.5}Ni_8Fe_2Be_{22.5}$  BAA, and 0.241 J/g·K for as-prepared  $Zr_{41}Ti_{14}Cu_{12.5}Ni_5Fe_5Be_{22.5}$  BAA when GT occurs. Johnson et al showed that the specific heat capacity transits from the glass to the supercooled liquid when the heating rate reaches  $1.67 \times 10^{-5}$  K/s in the case of  $Zr_{41.2}Ti_{13.8}Cu_{12.5}Ni_{10}Be_{22.5}$  BAA<sup>[10]</sup>. Therefore, the transformation from the glass to the supercooled liquid state of the BAA has the feature of the second-order phase transformation. Pre-annealing near  $T_g$  cannot change the feature. The glass transition process of the BMGs can be regarded as a kinetically modified phase transformation process.

Table 2 Values of  $A_0$  and  $B_0$  equation in Zr-based bulk amorphous alloys

Alloys	$T_g = A + B \ln \phi$		$T_x = A + B \ln \phi$		$T_{p1} = A + B \ln \phi$		$T_{p2} = A + B \ln \phi$	
	$A_g$	$B_g$	$A_x$	$B_x$	$A_{p1}$	$B_{p1}$	$A_{p2}$	$B_{p2}$
Zr <sub>41</sub> Ti <sub>14</sub> Cu <sub>12.5</sub> Ni <sub>10</sub> Be <sub>22.5</sub> (as-prepared)	612.49	5.68	645.31	21.86	664.93	20.68	698.10	15.66
Zr <sub>41</sub> Ti <sub>14</sub> Cu <sub>12.5</sub> Ni <sub>8</sub> Fe <sub>2</sub> Be <sub>22.5</sub> (as-prepared)	606.28	6.63	636.32	17.31	649.92	17.15	693.15	13.44
Zr <sub>41</sub> Ti <sub>14</sub> Cu <sub>12.5</sub> Ni <sub>5</sub> Fe <sub>3</sub> Be <sub>22.5</sub> (as-prepared)	617.27	5.39	646.83	13.81	659.00	14.76	697.74	13.08
Zr <sub>41</sub> Ti <sub>14</sub> Cu <sub>12.5</sub> Ni <sub>10</sub> Be <sub>22.5</sub> (annealed at 623K for 2 h)	610.00	7.00	630.04	19.11	664.25	15.31	699.94	13.74
Zr <sub>41</sub> Ti <sub>14</sub> Cu <sub>12.5</sub> Ni <sub>10</sub> Be <sub>22.5</sub> (annealed at 623 K for 6 h)	593.87	13.13	641.20	17.02	662.27	16.74	702.65	14.14

3.2 Glass forming ability and crystallization kinetics

In the process of preparing the Zr<sub>41</sub>Ti<sub>14</sub>Cu<sub>12.5</sub>Ni<sub>10-x</sub>Fe<sub>x</sub>Be<sub>22.5</sub> ( $x = 0, 2, 5$ ) BAAs, the cooling rate for the quenching is the same. The rate constant reflects GFA in some sense. According to Arrhenius law,  $\nu_T = \nu_0 \exp(-E/k_B T)$ , where  $\nu_T$  is crystallization rate constant at  $T$ , the atoms participating in the crystallization reaction will acquire additional energy to form an activated cluster<sup>[8]</sup>. This additional energy is captured through collisions. The activation energy  $E$  can be interpreted as the additional energy acquired by an atom before it becomes a part of the activated cluster. The frequency factor,  $\nu_0$ , is usually written as a product of two factors: atom collision probability and steric factor. According to Kissinger equation (1),  $\nu_0$  can be obtained from the

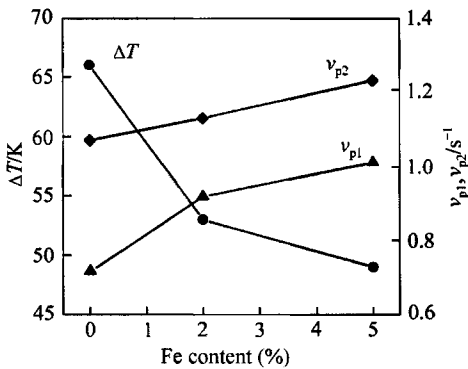


Fig. 5. Correlation of rate constant with the glass forming ability (represented by  $\Delta T$ ).

slope  $C$  and intercept  $D$  of Kissinger plots; that is,  $\nu_0 = C \exp(-D)$ . The crystallization rate constant at crystallization peak temperature,  $\nu_{pi}$ , can be calculated from the  $\nu_0$  and  $E$  of the corresponding crystallization peak. When the Fe content increases from 0 to 5%,  $\nu_{p1}$  are 0.007 17  $s^{-1}$ , 0.009 17  $s^{-1}$  and 0.010 1  $s^{-1}$ , and  $\nu_{p2}$  are 0.010 7  $s^{-1}$ , 0.011 3  $s^{-1}$  and 0.012 3  $s^{-1}$ . With the increasing Fe content,  $\nu_{pi}$  gradually increases, while the  $\Delta T$  gradually decreases. As has been shown above, the GFA of the BAAs can be represented by  $\Delta T$ , so the  $\nu_{pi}$  has a correlation with the GFA, (fig. 5). The BAA with smaller  $\nu_{pi}$  has a better GFA.

3.3 Effect of annealing-induced structural relaxation on glass transition and crystallization

Although BAAs is still in amorphous state after being annealed near  $T_g$ , the local atomic structure starts to change. The Zr<sub>41</sub>Ti<sub>14</sub>Cu<sub>12.5</sub>Ni<sub>10</sub>Be<sub>22.5</sub> BAA separates into two different amor-

phous phases when annealed in the region near  $T_g$  and the phase separation has a remarkable effect on subsequent crystallization<sup>[7]</sup>. In the process of annealing, structural relaxation, phase separation and nucleation occur in the BAA, changing the glass transition behavior and crystallization of the BAA. The as-prepared BAA must undergo a process of structure relaxation, phase separation, nucleation and growth of nuclei in the continuous heating. The  $E_g$  should include the activation energy of phase separations, relaxation and "real" GT. When the alloy is pre-annealed in the glass transition region, phase separations and relaxation have already occurred. So the  $E_g$  decreases, and it may reflect the pure glass transition process.

The crystallization process of an amorphous alloy comprises of the nucleation and growth of nuclei, and the  $E_{pi}$  derived from the Kissinger plots are the integration of the activation energy of nucleation and growth. The nucleation and growth of nuclei are closely related to the component diffusivity. The proceeding annealing near  $T_g$  will induce relaxation, decomposition, and formation of crystalline nuclei in the BAAs, and then change the subsequent nucleation process in continuous heating rate. The nucleation of as-prepared  $Zr_{41}Ti_{14}Cu_{12.5}Ni_{10}Be_{22.5}$  BAA are formed via a composition fluctuation from the initial homogeneous alloy, while the nucleation in the annealing BAA are formed in heterogeneous nucleation processes due to the heterogeneous structure and composition caused by phase separation. Meanwhile, the diffusion mechanisms and diffusivity in the conventional amorphous alloys is sensitive to the relaxation state of the samples, and the diffusivity in the relaxed alloy is smaller than that of the as-prepared alloy<sup>[11]</sup>. The apparent activation energy of crystallization in the  $Zr_{41}Ti_{14}Cu_{12.5}Ni_{10}Be_{22.5}$  bulk amorphous alloy increases after annealing in the region near  $T_g$ , suggesting that the annealing sample may probably have smaller diffusivity.

#### 4 Conclusions

(1) Both the glass transition and crystallization of Zr-based bulk amorphous alloys have kinetic effect. This feature cannot be changed by pre-annealing at  $T_g$ . The glass transition can be regarded as a kinetically modified phase transformation process.

(2) The glass-forming ability of Zr-based bulk amorphous alloys is related to the crystallization rate constant at crystallization peak temperature,  $\nu_{pi}$ . The bulk amorphous alloy with smaller  $\nu_{pi}$  has a higher glass forming ability.

(3) The glass transition and crystallization of annealing samples are different from those of the corresponding as-prepared bulk amorphous alloys. The annealing alloys have smaller values of apparent activation energy of glass transition and greater values of apparent activation energy of crystallization than the as-prepared alloys.

**Acknowledgements** The authors would like to thank Prof. K. Q. Lu and Prof. X. C. Chen for their valuable suggestions and help. This work was supported by the National Natural Science Foundation of China (Grant No. 59871059).

#### References

1. Peker, A., Johnson, W. L., A highly processably metallic glass:  $Zr_{41.2}Ti_{13.8}Cu_{12.5}Ni_{10.0}Be_{22.5}$ , Appl. Phys. Lett., 1993,

- 63: 2342.
2. Wang Weihua, Wang Wenkui, Bai Hai Yang, Formation of New Zr-Ti-Cu-Ni-Be-C bulk amorphous alloys, Science in China (in Chinese), Ser. A, 1998, 28: 443.
  3. Inoue, A., Zhang, T., Nishiyama, N. et al., Preparation of 16 mm diameter rod of amorphous  $Zr_{65}Al_{7.5}Ni_{10}Cu_{17.5}$  alloy, Mater. Trans. JIM, 1993, 34: 1234.
  4. Shen, T. D., Schwarz, R. B., Bulk ferromagnetic glasses prepared by flux melting and water quenching, Appl. Phys. Lett., 1999, 75: 49.
  5. Kelton, K. F., A new model for nucleation in bulk metallic glasses, Phil. Mag. Lett., 1998, 77: 337.
  6. Tsao, S. S., Spaepen, F., Structural relaxation of a metallic glass near equilibrium, Acta Metall., 1989, 33: 881.
  7. Wang, W. H., Wei, Q., Friedrich, S., Microstructure, decomposition, and crystallization in  $Zr_{41}Ti_{14}Cu_{12.5}Ni_{10}Be_{22.5}$  bulk metallic glass, Phys. Rev. B, 1998, 57: 8211.
  8. Kissinger, H. E., Variation of peak temperature with heating rate in differential thermal analysis, J. Res. Nat. Bur. St., 1956, 57: 217.
  9. Inoue, A., High strength bulk amorphous alloys with low critical cooling rates, Mater. Trans. JIM, 1995, 36: 866.
  10. Busch, R., Kim, Y. J., Johnson, W. L., Thermodynamic and kinetics of the undercooled liquid and the glass transition of the  $Zr_{41.2}Ti_{13.8}Cu_{12.5}Ni_{10.0}Be_{22.5}$  alloy, J. Appl. Phys., 1995, 77: 4039.
  11. Frank, W., Hörner, A., Scharwaechter, P. et al., Diffusion in amorphous metallic alloys, Mater. Sci. Eng. A, 1994, 179/180: 36.